Advances in Computational Design, *Vol. 10, No. 2 (2025) 151-167*
https://doi.org/10.12989/acd.2025.10.2.151

New analytical method for optimum design of circular and elliptical footings

Mohamed Elhanash*[1], Ahmed K. Elsherif[1a], AlHaytham Aref[1b] and Nabil M. Nagy[2c]

[1]*Department of Mathematics, Military Technical College, Cairo, Egypt*
[2]*Department of Civil Engineering, Military Technical College, Cairo, Egypt*

(Received March 12, 2025, Revised April 18, 2025, Accepted April 21, 2025)

Abstract. This research presents a new mathematical framework for the optimal design of elliptical isolated footings under vertical load and two orthogonal moments. The suggested method considers the spatial variation of contact pressure between the footing and the supporting soil, facilitating an accurate representation of structural requirements. New formulations for bending moment, unidirectional shear, and punching shear are generated using volume integration, accurately representing the complex stress distribution beneath elliptical foundations. Lagrange multipliers are utilized to identify the crucial points of maximum and minimum contact stresses for elliptical and circular footing shapes. A thorough numerical analysis illustrates the benefits of the suggested strategy by contrasting its results with those of a conventional design methodology. The findings demonstrate that the newly created model produces more cost-effective designs while maintaining structural integrity and performance, underscoring its potential as a significant asset in engineering practice. A MATLAB code for design using new formulas is programmed and results obtained compared to those from literature and were more efficient and economic.

Keywords: contact pressure; circular footing; elliptical footing; optimum design

1. Introduction

Foundation is the fundamental structural component that effectively transfers loads and moments to the soil (Bowles 2001). Foundations are classified into many types according to their depth, geometry, and function. They are classified by depth into shallow and deep types and further differentiated by geometry such as square, rectangular, circular, etc. Shallow foundations vary based on functionality, including isolated, combined, mat, and strip foundations. The contact pressure between the soil and the ground significantly influences design objectives. The pressure distribution beneath the foundation surface is affected by several factors, including the relative rigidity of the foundation in relation to the soil's bottom and the foundation's depth. The classical design method assumes that the homogeneous linear pressure is maximized at all contact surface

*Corresponding author, MSc. Student, E-mail: elhanash@mtc.edu.eg
[a] Ph.D., E-mail: aelsherif@mtc.edu.eg
[b] Ph.D., E-mail: H.aref@mtc.edu.eg
[c] Professor, E-mail: nnagy@mtc.edu.eg

 ISSN: 2383-8477 (Print), 2466-0523 (Online)

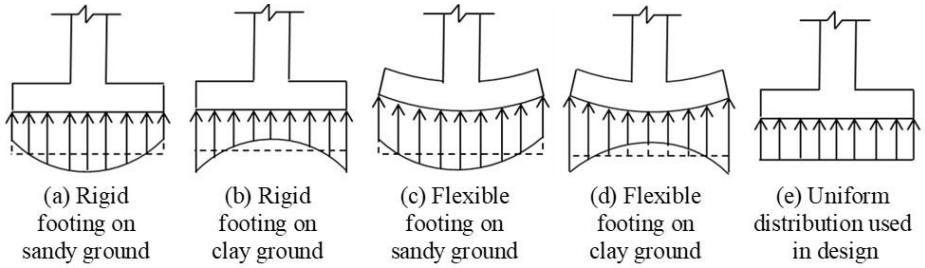

Fig. 1 Contact pressure distributions for various types of soil and footings

points (Reese *et al*. 2006). The conventional approach has examined the most prevalent shapes of shallow reinforced concrete footings, specifically square and rectangular shapes (Elhanash *et al*. 2023, Luévanos-Rojas *et al*. 2024). Few studies have been conducted to examine the design of irregular footing forms such as trapezoidal, triangular and T-shaped (Al-Ansari and Afzal 2021, Rojas *et al*. 2018). Traditional design methodology fails to incorporate the actual soil pressure; instead, it assumes a maximum pressure distribution beneath the contact surface. This assumption results in enlarged dimensions and higher steel reinforcement, thereby increasing building expenses. Contact pressure between footing and soil varies according to soil nature and rigidity of soil and footing as shown in Fig. 1. Many researchers have recommended considering the actual pressure at every point of contact (Landeros *et al*. 2024). A methodology for calculating the ultimate bearing capacity of shallow footings in unsaturated soils has been presented, taking into account site-specific climatic and geotechnical factors (Ravichandran *et al*. 2017). A comparative analysis of partial safety factors and comprehensive probabilistic approaches is provided in (Vořechovský *et al*. 2024). Finite element methods have been employed to model the rocking behavior of shallow foundations subjected to slow cyclic loads, highlighting the significance of soil-structure interaction (Haeri and Fathi 2015). Additionally, deep neural networks have been applied to forecast the eventual bearing capacity of shallow foundations, particularly in cases with limited experimental data (Bagińska and Srokosz 2019). Influence of depth of isolated footing had been investigated (Mittal *et al*. 2024). Many authors have investigated the behavior and design of circular footings under different loading and soil conditions (Kim-Sánchez *et al*. 2022, López-Chavarría *et al*. 2019, Luévanos-Rojas 2016). Several studies had been performed to minimize construction costs and produce economical designs of isolated footing (Babu and Ibrahim 2023, Nawaz *et al.* 2022). In this paper, the position of maximum and minimum stress of circular and elliptical foundations subjected to a vertical load and two orthogonal moments is derived. A new analytical method is proposed to examine the effect of moments and load on the design of elliptical and circular isolated footings. A general formula for the critical sections of moments, unidirectional shear, and bidirectional shear force is obtained using the volume of pressure.

2. Methedology

2.1 Circular footing on rigid medium

A rigid RC circular footing with radius “R” and thickness “T” subjected to two orthogonal

moments (around the x-axis and y-axis) and a vertical load P, rests on rigid soil see Fig. 2. Contact pressure is assumed to be linear at all points of contact between the soil and the bottom surface of the footing. For a vertical load and two orthogonal moments of a circular isolated footing, the stress $\sigma(x, y)$ at any point on the contact surface is given by (Bowels 2001):

$$\sigma(x,y) = \frac{P}{A} \pm \frac{M_x}{I_x} y \pm \frac{M_y}{I_y} x \tag{1}$$

Here, P represents total vertical axial unfactored load, A represents area of isolated footing, M_x and M_y represent moments around x and y directions, respectively. I_x and I_y are moments of inertia about x and t directions, respectively. To determine positions of maximum and minimum stress on the boundary $x^2 + y^2 = R^2$, we apply the Lagrange multipliers technique (Boyd and Vandenberghe 2004, Zhai 2024) with the constraint:

$$g(x,y) = x^2 + y^2 = R^2 \tag{2}$$

$$\nabla_{x,y}\sigma(x,y) = \lambda \nabla_{x,y} g(x,y) \tag{3}$$

where

$$\nabla_{x,y} = \left(\frac{\partial}{\partial x}, \frac{\partial}{\partial y}\right) \tag{4}$$

Here, (x, y) are any points lies on the boundary of circular footing, r is the radius of footing. Substituting in equation (3):

$$\frac{M_y}{Iy} = 2\lambda x \tag{5}$$

$$\frac{M_x}{Ix} = 2\lambda y \tag{6}$$

The resultant moment M_R in case of circular rigid footing subjected to linear uniform pressure at contact surface is:

$$M_R = \sqrt{{M_x}^2 + {M_y}^2} \tag{7}$$

Substituting from equation (7) into equations (5) and (6)

$$x = \pm \frac{M_y}{\sqrt{{M_y}^2 + {M_x}^2}} R \tag{8}$$

$$y = \pm \frac{M_x}{\sqrt{{M_y}^2 + {M_x}^2}} R \tag{9}$$

Values of (x, y) obtained in equations (8) and (9) determine position of maximum and minimum stress on the boundary of rigid circular footing.

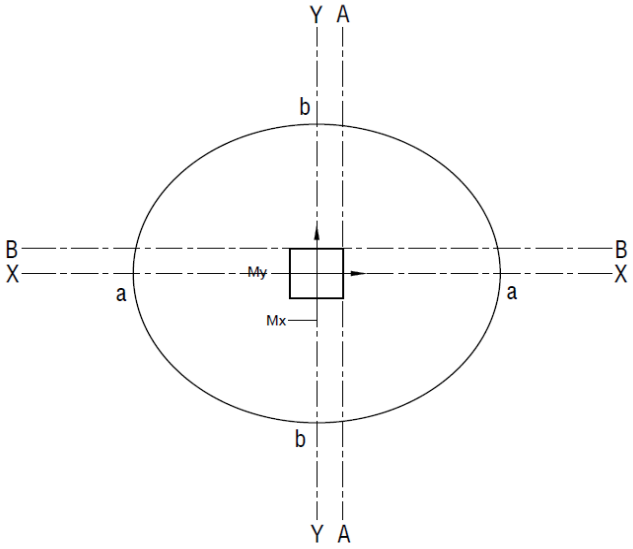

Fig. 2 Elliptical footing with semi-axes a and b subjected to vertical load and two orthogonal moments

2.2 Elliptical footing on rigid medium

For an elliptical footing resting on a rigid medium and assuming a uniform linear pressure at the contact surface, the boundary is given by:

$$g(x,y) = \frac{x^2}{a^2} + \frac{y^2}{b^2} \tag{10}$$

Then, following the same procedure, the ordered pairs (x, y) are derived as:

$$x = \pm \frac{abM_y}{\sqrt{b^2{M_y}^2 + a^2{M_x}^2}} \tag{11}$$

$$y = \pm \frac{abM_x}{\sqrt{b^2{M_y}^2 + a^2{M_x}^2}} \tag{12}$$

3. Elliptical footing

3.1 Critical sections for moments

Critical sections of moments for an elliptical isolated footing occur at the column face, as shown in Fig. 2.

To evaluate the moment about the A–A axis, the resultant force of pressure from the column face to the edge of the footing is calculated as:

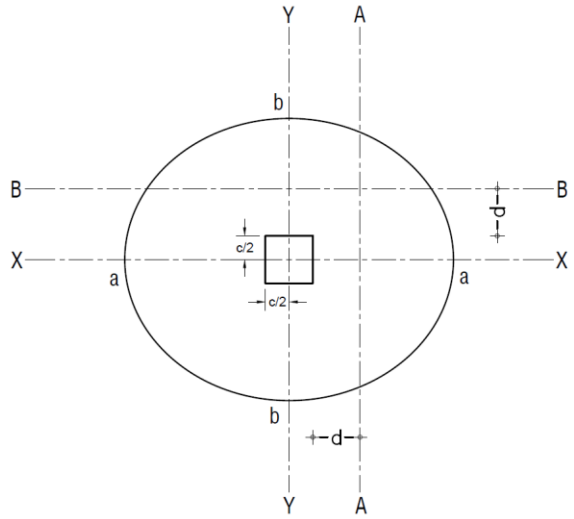

Fig. 3 Critical sections of unidirectional shear in both directions at distance d from column face.

$$F_1 = \frac{1}{\pi ab}\int_{\frac{c}{2}}^{a}\int_{-b\sqrt{1-\frac{x^2}{a^2}}}^{b\sqrt{1-\frac{x^2}{a^2}}} P + \frac{4M_x}{b^2}y + \frac{4M_y}{a^2}x \, dy \, dx \tag{13}$$

This expression simplifies to:

$$F_1 = \frac{3a^4P[\frac{\pi - \sin\left(2\arcsin\left(\frac{c}{2a}\right)\right)}{2} - \arcsin\left(\frac{c}{2a}\right)] + M_y(4a^2 - c^2)^{\frac{3}{2}}}{3\pi a^4} \tag{14}$$

The centroid along the x-axis is defined as

$$X_c = \frac{\int\int_D x\sigma(x,y)\,dA}{\int\int_D \sigma(x,y)\,dA} = \frac{\int_{\frac{c}{2}}^{a}\int_{-b\sqrt{1-\frac{x^2}{a^2}}}^{b\sqrt{1-\frac{x^2}{a^2}}}\left(\frac{P}{A} + \frac{4M_x}{b^2}y + \frac{4M_y}{a^2}x\right)x\,dy\,dx}{\int_{\frac{c}{2}}^{a}\int_{-b\sqrt{1-\frac{x^2}{a^2}}}^{b\sqrt{1-\frac{x^2}{a^2}}}\frac{P}{A} + \frac{4M_x}{b^2}y + \frac{4M_y}{a^2}x\,dy\,dx} \tag{15}$$

This further simplifies to:

$$X_c = \frac{a^2[P(4a^2 - c^2)^{\frac{3}{2}} + 3M_y a^2\left(\sin\left(4\arcsin\left(\frac{c}{2a}\right)\right) + 2\pi - 4\arcsin\left(\frac{c}{2a}\right)\right)]}{2[3a^4P\left(\pi - 2\arcsin\left(\frac{c}{2a}\right) - \sin\left(2\arcsin\left(\frac{c}{2a}\right)\right)\right) + 2M_y(4a^2 - c^2)^{\frac{3}{2}}]} \tag{16}$$

Then the moment about the A–A axis is given by:

$$M_{A-A} = F_1 * (X_c - \frac{c}{2}) \tag{17}$$

Similarly, moment around column face at Sec (B-B) can be obtained using same procedures:

$$F_2 = \frac{1}{\pi ab}\int_{\frac{c}{2}}^{b}\int_{-a\sqrt{1-\frac{y^2}{b^2}}}^{a\sqrt{1-\frac{y^2}{b^2}}} P + \frac{4M_x}{b^2}y + \frac{4M_y}{a^2}x\,dx\,dy \tag{18}$$

which simplifies to:

$$F_2 = \frac{3b^4P[\frac{\pi - sin\left(2\,arcsin\left(\frac{c}{2b}\right)\right)}{2} - arcsin\left(\frac{c}{2b}\right)] + M_x(4b^2 - c^2)^{\frac{3}{2}}}{3\pi b^4} \tag{19}$$

The centroid along the y-axis is defined by:

$$y_c = \frac{\int\int_D y\sigma(x,y)\,dA}{\int\int_D \sigma(x,y)\,dA} = \frac{\int_{\frac{c}{2}}^{b}\int_{-a\sqrt{1-\frac{y^2}{b^2}}}^{a\sqrt{1-\frac{y^2}{b^2}}} (P + \frac{4M_x}{b^2}y + \frac{4M_y}{a^2}x)y\,dx\,dy}{\int_{\frac{c}{2}}^{b}\int_{-a\sqrt{1-\frac{y^2}{b^2}}}^{a\sqrt{1-\frac{y^2}{b^2}}} P + \frac{4M_x}{b^2}y + \frac{4M_y}{a^2}x\,dx\,dy} \tag{20}$$

$$y_c = \frac{b^2[P(4b^2 - c^2)^{\frac{3}{2}} + 3M_xb^2\left(\sin\left(4\arcsin\left(\frac{c}{2b}\right)\right) + 2\pi - 4\arcsin\left(\frac{c}{2b}\right)\right)]}{2[3b^4P\left(\pi - 2\arcsin\left(\frac{c}{2b}\right) - \sin\left(2\arcsin\left(\frac{c}{2b}\right)\right)\right) + 2M_x(4b^2 - c^2)^{\frac{3}{2}}]} \tag{21}$$

Then the moment about section B–B is given by:

$$M_{B-B} = F_2 * (y_c - \frac{c}{2}) \tag{22}$$

3.2 Critical sections for unidirectional shear and punching

Critical section for unidirectional shear occurs at distance d from the column face as shown in Fig. 3.

The unidirectional shear force for section (e-e) is given by

$$V_{e-e} = \frac{1}{\pi ab}\int_{\frac{c}{2}+d}^{a}\int_{-b\sqrt{1-\frac{x^2}{a^2}}}^{b\sqrt{1-\frac{x^2}{a^2}}} P + \frac{4M_x}{b^2}y + \frac{4M_y}{a^2}x\,dydx \tag{23}$$

$$V_{e-e} = \frac{3a^4P[\frac{\pi - \sin\left(2\arcsin\left(\frac{c+2d}{2a}\right)\right)}{2} - \arcsin\left(\frac{c+2d}{2a}\right)] + M_y(-4d^2 - 4dc + 4a^2 - c^2)^{\frac{3}{2}}}{3\pi a^4} \tag{24}$$

For section (f–f):

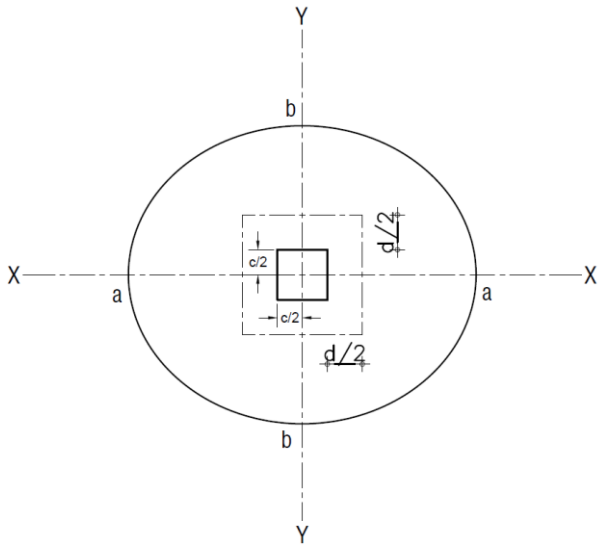

Fig. 4 Critical sections of bidirectional shear at distance d/2 from column face

$$V_{f-f} = \frac{1}{\pi ab} \int_{\frac{c}{2}+d}^{b} \int_{-a\sqrt{1-\frac{y^2}{b^2}}}^{a\sqrt{1-\frac{y^2}{b^2}}} P + \frac{4M_x}{b^2} y + \frac{4M_y}{a^2} x \, dxdy \tag{25}$$

$$V_{f-f} = \frac{3b^4 P[\frac{\pi - \sin\left(2\arcsin\left(\frac{c+2d}{2b}\right)\right)}{2} - \arcsin\left(\frac{c+2d}{2b}\right)] + Mx(-4d^2 - 4dc + 4b^2 - c^2)^{\frac{3}{2}}}{3\pi b^4} \tag{26}$$

For punching shear force at distance d/2 from the column face as shown in Fig. 4.

$$Q = P - \frac{1}{\pi ab} \int_{-\frac{c}{2}-\frac{d}{2}}^{\frac{c}{2}+\frac{d}{2}} \int_{-\frac{c}{2}-\frac{d}{2}}^{\frac{c}{2}+\frac{d}{2}} P + \frac{4M_x}{b^2} y + \frac{4M_y}{a^2} x \, dx \, dy \tag{27}$$

$$Q = P - \frac{P(c^2 + 2cd + d^2)}{\pi ab} \tag{28}$$

4. Circular footing

For a circular footing (i.e., a = b = R), the previous equations reduce accordingly (Rojas 2014). For example, for section (A–A):

$$F_1 = \frac{1}{\pi R^2} \int_{\frac{c}{2}}^{R} \int_{-\sqrt{R^2-x^2}}^{\sqrt{R^2-x^2}} P + \frac{4M_x}{R^2} y + \frac{4M_y}{R^2} x \, dy \, dx \tag{29}$$

$$F_1 = \frac{3R^4P[\frac{\pi - \sin\left(2\arcsin\left(\frac{c}{2R}\right)\right)}{2} - \arcsin\left(\frac{c}{2R}\right)] + M_y(4R^2 - c^2)^{\frac{3}{2}}}{3\pi R^4} \tag{30}$$

$$X_c = \frac{\int\int_D x\sigma(x,y)\, dA}{\int\int_D \sigma(x,y)\, dA} = \frac{\int_{\frac{c}{2}}^{R} \int_{-\sqrt{R^2-x^2}}^{\sqrt{R^2-x^2}} (P + \frac{4M_x}{R^2} y + \frac{4M_y}{R^2} x) x \, dy \, dx}{\int_{\frac{c}{2}}^{R} \int_{-\sqrt{R^2-x^2}}^{\sqrt{R^2-x^2}} P + \frac{4M_x}{R^2} y + \frac{4M_y}{R^2} x \, dy \, dx} \tag{31}$$

$$X_c = \frac{R^2[P(4R^2 - c^2)^{\frac{3}{2}} + 3M_y R^2 \left(\sin\left(4\arcsin\left(\frac{c}{2R}\right)\right) + 2\pi - 4\arcsin\left(\frac{c}{2R}\right)\right)]}{2[3R^4P\left(\pi - 2\arcsin\left(\frac{c}{2R}\right) - \sin\left(2\arcsin\left(\frac{c}{2R}\right)\right)\right) + 2M_y(4R^2 - c^2)^{\frac{3}{2}}]} \tag{32}$$

$$M_{A-A} = F_1 * (X_c - \frac{c}{2}) \tag{33}$$

$$F_2 = \frac{1}{\pi R^2} \int_{\frac{c}{2}}^{R} \int_{-\sqrt{R^2-y^2}}^{\sqrt{R^2-y^2}} P + \frac{4M_x}{R^2} y + \frac{4M_y}{R^2} x \, dx dy \tag{34}$$

$$F_2 = \frac{3R^4P[\frac{\pi - \sin\left(2\arcsin\left(\frac{c}{2R}\right)\right)}{2} - \arcsin\left(\frac{c}{2R}\right)] + M_x(4R^2 - c^2)^{\frac{3}{2}}}{3\pi R^4} \tag{35}$$

$$y_c = \frac{\int\int_D y\sigma(x,y)\, dA}{\int\int_D \sigma(x,y)\, dA} = \frac{\int_{\frac{c}{2}}^{R} \int_{-\sqrt{R^2-y^2}}^{\sqrt{R^2-y^2}} (P + \frac{4M_x}{R^2} y + \frac{4M_y}{R^2} x) y \, dx dy}{\int_{\frac{c}{2}}^{R} \int_{-\sqrt{R^2-y^2}}^{\sqrt{R^2-y^2}} P + \frac{4M_x}{R^2} y + \frac{4M_y}{R^2} x \, dx dy} \tag{36}$$

$$y_c = \frac{R^2[P(4R^2 - c^2)^{\frac{3}{2}} + 3M_x R^2 \left(\sin\left(4\arcsin\left(\frac{c}{2R}\right)\right) + 2\pi - 4\arcsin\left(\frac{c}{2R}\right)\right)]}{2[3R^4P\left(\pi - 2\arcsin\left(\frac{c}{2R}\right) - \sin\left(2\arcsin\left(\frac{c}{2R}\right)\right)\right) + 2M_x(4R^2 - c^2)^{\frac{3}{2}}]} \tag{37}$$

$$M_{B-B} = F_2 * (y_c - \frac{c}{2}) \tag{38}$$

For section (e-e):

$$V_{e-e} = \frac{1}{\pi R^2} \int_{\frac{c}{2}+d}^{R} \int_{-\sqrt{R^2-x^2}}^{\sqrt{R^2-x^2}} P + \frac{4M_x}{R^2} y + \frac{4M_y}{R^2} x \, dydx \tag{39}$$

$$V_{e-e} = \frac{3R^4 P[\frac{\pi - \sin\left(2\arcsin\left(\frac{c+2d}{2R}\right)\right)}{2} - \arcsin\left(\frac{c+2d}{2R}\right)] + M_y(-4d^2 - 4dc + 4R^2 - c^2)^{\frac{3}{2}}}{3\pi R^4} \tag{40}$$

For section (f-f):

$$V_{f-f} = \frac{1}{\pi R^2} \int_{\frac{c}{2}+d}^{R} \int_{\sqrt{R^2-y^2}}^{\sqrt{R^2-y^2}} P + \frac{4M_x}{R^2} y + \frac{4M_y}{R^2} x \, dxdy \tag{41}$$

$$V_{f-f} = \frac{3R^4 P[\frac{\pi - \sin\left(2\arcsin\left(\frac{c+2d}{2R}\right)\right)}{2} - \arcsin\left(\frac{c+2d}{2R}\right)] + M_x(-4d^2 - 4dc + 4R^2 - c^2)^{\frac{3}{2}}}{3\pi R^4} \tag{42}$$

For punching shear force:

$$Q = P - \frac{1}{\pi R^2} \int_{-\frac{c}{2}-\frac{d}{2}}^{\frac{c}{2}+\frac{d}{2}} \int_{-\frac{c}{2}-\frac{d}{2}}^{\frac{c}{2}+\frac{d}{2}} P + \frac{4Mx}{R^2} y + \frac{4My}{R^2} x \, dxdy \tag{43}$$

$$Q = P - \frac{P(c^2 + 2cd + d^2)}{\pi R^2} \tag{44}$$

5. Numerical study

A parametric study has been conducted to validate the accuracy of the new moment and shear equations for the optimum design of isolated footings according to (ACI 318). Table 1 shows different circular footings (F1–F7) with different load conditions (AlAnsari and Afzal 2021).

The following input parameters were used for the design:

$f_y = 400$ MPa $\quad \gamma_c = 25$ KN/m^3 $\quad D_f = 1$ m $\quad d' = 0.075$ m

$f_c = 30$ MPa $\quad \gamma_s = 15$ KN/m^3 $\quad Q_a = 200$ KPa

Here, f_y represents reinforcement yield strength, γ_c represents self weight of concrete, D_f is the depth of footing, d' is the concrete cover, f_c represents concrete compressive strength, γ_s represents self weight of soil, and Q_a is the allowable soil bearing capacity. A MATLAB code is

Table 1 Seven footings with different load conditions

Footing	P_D(KN)	P_L(KN)	M_{Dx}(KN.m)	M_{lx}(KN.m)	M_{Dy}(KN.m)	M_{ly}(KN.m)	Col.(cm*cm)
F_1	200	100	18	24	12	16	30*30
F_2	120	70	9	12	15	20	27*27
F_3	1000	800	60	80	45	60	50*50
F_4	500	200	27	36	15	20	32*32
F_5	2000	1300	45	60	75	100	55*55
F_6	800	600	30	40	9	12	35*35
F_7	3000	2000	185	80	120	85	70*70

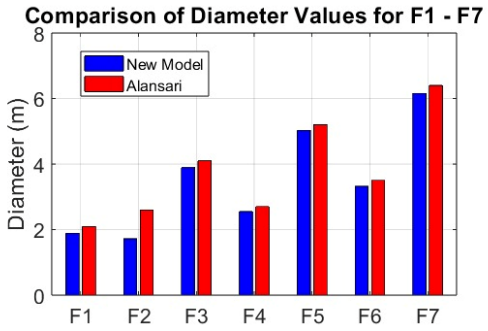

Fig. 5 Comparison between diameter of seven different isolated circular footings

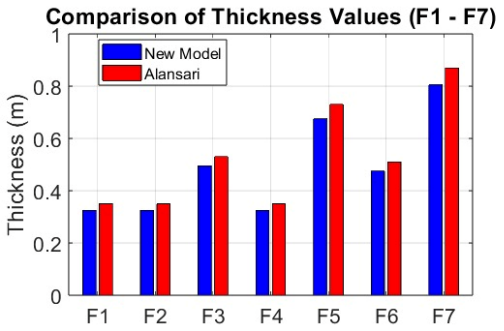

Fig. 6 Comparison between thickness of seven different isolated circular footings

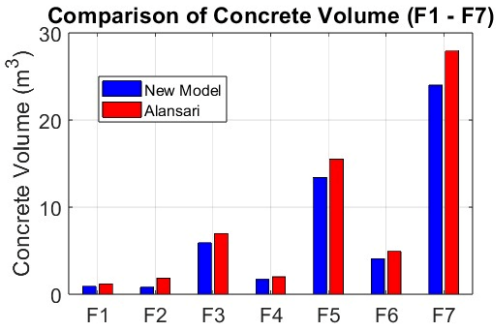

Fig. 7 Comparison between overall volume of all seven different circular footings

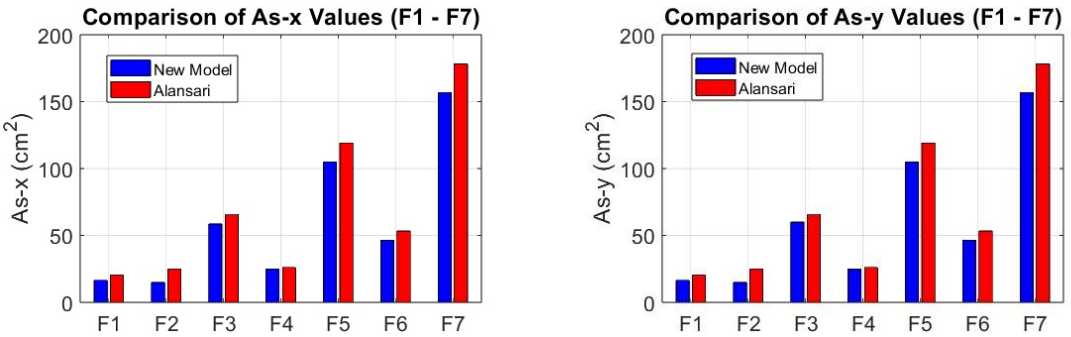

(a) A_{sx} (b) A_{sy}

Fig. 8 Comparison between area steel in both directions

programmed to determine the concrete dimensions, steel area in both directions, as well as shear and moment values, as shown in Appendix. Appendix show case study of F_3 and by changing load conditions; dimensions and area steel of other footings can be obtained.

6. Results

The below figures show comparisons between different results obtained from the new method.

As shown in Fig. 5 for all seven cases, the proposed method is more economical as it produces smaller diameters compared to those from literature. Similarly, the total thickness of concrete is lower than the traditional method see Fig. 6. Hence, the new analytical method suggests lower cost of concrete compared to traditional methods see Fig. 7. Fig. 8 shows comparison between area steel in both directions (In our case author consider reinforcement in orthogonal directions not radial). It's clear that the new analytical method produces less area of steel in all cases of study, Hence it's more economical. Equations of elliptical footing for critical sections of moments, shear and punching reduced to those of circular footing when considering both sides are equal. Also position of maximum and minimum stress of elliptical footing is the same for circular when considering same inertia for x and y direction.

7. Conclusions

Foundation is the main essential part that transmits load safely to the soil. The classical method of design assumes maximum contact pressure under the concrete footing, which results in high cost due to larger concrete dimensions and increased steel area. A new method considers variation of pressure at every single point rather than dealing with maximum pressure. The goals of this paper are summarized as follows:

• Position of maximum and minimum contact pressure under elliptical and circular footings subjected to vertical load and two orthogonal moments is presented using Lagrange multipliers.

• New analytical method for the design of isolated elliptical footings subjected to vertical load and two orthogonal moments is presented. The method uses the volume of pressure to derive moments at critical sections and develops equations for unidirectional shear and punching shear.

• Comparative study with literature for seven different isolated circular footings demonstrates that the proposed method provides more realistic and economical designs. The model described in this study assumes linear elastic behavior of soil and assumes rigidity of supported footings.

• A matlab code is programmed for design circular isolated footing according to ACI code. Input parameters include dead load, live load, dead and live moments around x and y axis. Also, depth of footing, Self weight of soil and concrete, concrete cover and reinforcement yield strength. By running matlab model; Initial depth is assumed and net allowable bearing capacity is calculated then calculating radius of concrete footing according to code requirements. Then, Ultimate applied load and moments are calculated and substituting in new formulas of moment and shear equations, Comparing these results with allowable values from code. If applied values are higher than allowable ones, Iterations for increasing depth is processed. If shear requirements are satisfied, Area steel in x and y direction is calculated and taking into consideration minimum steel area requirement.

Acknowledgments

I like to express my profound appreciation to the editor and the anonymous reviewers for their invaluable feedback and insightful recommendations, which have markedly enhanced the quality of this paper. Their direction and constructive feedback have refined the text and ensured clarity in presenting the findings. I sincerely value their time and effort in evaluating this work.

References

ACI 318 (2011), *Building Code Requirements for Structural Concrete and Commentary*, American Concrete Institute, Farmington Hills, MI, U.S.A.

Al-Ansari, M. and Afzal, M.S. (2021), "Structural analysis and design of irregular shaped footings subjected to eccentric loading", *Eng. Reports*, **3**(1), 1-17. https://doi.org/10.1002/eng2.12283

Babu, T.S. and Ibrahim, S.K.N. (2023), "Design of circular footings considering soil-structure interaction". *AIP Conf. Proc.*, **2810**(1), 070002. https://doi.org/10.1063/5.0147532

Bagińska, A. and Srokosz, P.E. (2019), "The optimal ann model for predicting bearing capacity of shallow foundations trained on scarce data", *KSCE J. Civ. Eng.*, **23**(1), 130-137. https://doi.org/10.1007/s12205-018-2636-4

Bowles, J.E. (2001), *Foundation Analysis and Design*, (5th Edition), McGraw-Hill, New York, NY, U.S.A.

Boyd, S. and Vandenberghe, L. (2004), *Convex Optimization*, Cambridge University Press, New York, NY, U.S.A.

Elhanash, M., Elsherif, A.K., Zaky, H.N. and Nagy, N.M. (2023), "A new mathematical model to evaluate the effect of load inclination on aircraft shelter's foundations", *J. Phys. Conf. Ser.*, **2616**(1), 012050. https://doi.org/10.1088/1742-6596/2616/1/012050

Haeri, H. and Fathi, A. (2015), "Numerical modeling of rocking of shallow foundations subjected to slow cyclic loading with consideration of soil-structure interaction", *Proceedings of the Fifth International Conference on Geotechnique, Construction Materials and Environment*, Osaka, Japan, November.

Kim-Sanchez, D.S., Luévanos-Rojas, A., Barquero-Cabrero, J.D., López-Chavarría, S., Medina-Elizondo, M., Luévanos-Soto, I. (2022), "A new model for the complete design of circular isolated footings considering that the contact surface works partially under compression", *Int. J. Innov. Comput. Inform. Control*, **18**(6), 1769-1784. https://doi.org/10.24507/ijicic.18.06.1769

Landeros, A.L., Rojas, G.S., Hurtado, L., León, L.D., Diaz-Gurrola, E.R., Coca, F.J., León, A.L., and

Gomez, A.E. (2024), "Optimal area for a rectangular isolated footing with an eccentric column and partial ground compression", *Appl. Sci.*, **14**(15), 6453. https://doi.org/10.3390/app14156453
Landeros, A.L., Rojas, G.S., Hurtado, L., León, F.J., Coca, F.J., León, A.L., and Gomez, A.E. (2024), "Optimal cost design of rc t-shaped combined footings", *Buildings*, **14**(11), 3688. https://doi.org/10.3390/buildings14113688
López-Chavarría, S., Luévanos-Rojas, A., Medina-Elizondo, M., Ricardo Sandoval-Rivas, R., Velázquez-Santillán, F. (2019), "Optimal design for the reinforced concrete circular isolated Footings", *Adv. Comput. Des.* **4**(3), 273-294. https://doi.org/10.12989/acd.2019.4.3.273
Luévanos Rojas, A. (2016), "A comparative study for the design of rectangular and circular isolated footingsusing new models", *Dyna*, **83**(196), 149-158. https://doi.org/10.15446/dyna.v83n196.51056
Luévanos-Rojas, A., Lopez-Chavarria, S. and Medina-Elizondo, M. (2018), "A new model for t-shaped combined footings part i: optimal dimensioning", *Geomech.Eng.*, **14**(1), 51-60. https://doi.org/10.12989/gae.2018.14.1.051
Mittal, M., Samanta, M., and Kanungo, D.P.(2024) "Influence of isolated footing embedment on the seismic performance of building considering the soil foundation structure interaction: An experimental approach", *J. Rock Mech. Geotech. Eng.*, **17**(2), 1194-1212. https://doi.org/10.1016/j.jrmge.2024.04.019
Nawaz, M.N., Ali, A.S., Jaffar, S.T.A., Jafri, T.H., Oh, T.M., Abdallah, M., Karam, S. and Azab, M. (2022), "Cost-based optimization of isolated footing in cohesive soils using generalized reduced gradient method", *Buildings*, **12**(10), 1646. https://doi.org/10.3390/buildings12101646
Ravichandran, V., Mahmoudabadi, S., and Shrestha, S. (2017), "Analysis of the bearing capacity of shallow foundation in unsaturated soil using monte carlo simulation", *Int. J. Geosci.*, **8**(10), 1231-1250. https://doi.org/10.4236/ijg.2017.810071
Reese, L.C., Isenhower, W.M., and Wang, S.T. (2006), *Analysis and Design of Shallow and Deep Foundations*, John Wiley, Hoboken, NJ, U.S.A.
Rojas, A.L. (2014), "Design of isolated footings of circular form using a new model", *Struct. Eng. Mech.*, **52**(4), 767-786. https://doi.org/10.12989/sem.2014.52.4.767
Vořechovský, L., Miča, L., and Boštík, J. (2024), "Shallow foundation design: a comparative study of partial safety factors and full probabilistic methods", *Sci. Rep.*, **14**(1), 1-11. https://doi.org/10.1038/s41598-024-63003-0
Zhai, J. (2024), "An introduction to lagrange multipliers: theory and applications in economics", *Dean Francis Academic Publ.*, **1**(9). https://doi.org/10.61173/ch4v0m11

CC

Appendix

```
function F3
    clc;

    %% ------------------------------------------------------
    % 1) DEFINE INPUTS (Column, Loads, Soil, Material)
    %% ------------------------------------------------------
    % Column properties
    c = 0.5;                % m, square column side length

    % Axial loads (kN)
    P_dead = 1000;          % kN, dead load
    P_live = 800;           % kN, live load
```

```
% Moments (kN·m)
Mx_dead = 60;         % kN·m, dead moment about X
Mx_live = 80;        % kN·m, live moment about X
My_dead = 45;        % kN·m, dead moment about Y
My_live = 60;         % kN·m, live moment about Y

% Soil properties
qa = 200;                % kN/m², allowable soil bearing capacity
gamma_soil = 15;    % kN/m³ (overburden soil unit weight)

% Material properties
fc = 30;                  % MPa, concrete compressive strength
fy = 400;                % MPa, reinforcement yield strength
cover = 0.075;        % m, concrete cover

%% ---------------------------------------------------
% 2) CALCULATE TOTAL UNFACTORED LOADS
%% ---------------------------------------------------
P_total = P_dead + P_live;                          % kN
Mx_total = Mx_dead + Mx_live;                     % kN·m
My_total = My_dead + My_live;                     % kN·m
M_combined = sqrt(Mx_total^2 + My_total^2);    % kN·m

%% ---------------------------------------------------
% 3) INITIAL FOOTING RADIUS (R) CALCULATION
%% ---------------------------------------------------
gamma_concrete = 24;    % kN/m³
d_init = 0.25;               % m, initial guess for effective depth
h0 = d_init + cover;
gamma_ppz = gamma_concrete * h0;                % kN/m²
gamma_pps = gamma_soil * (1-h0);                   % kN/m² (1.5 m overburden)
sigma_max = qa - gamma_ppz - gamma_pps;      % kN/m²

% Solve for R using cubic equation
syms R_sym
eqn = sigma_max*pi*R_sym^3 - P_total*R_sym - 4*M_combined == 0;
R_guess = (4 * M_combined) / P_total;        % Initial guess
R_sol = double(vpasolve(eqn, R_sym, R_guess));
R_sol = R_sol(R_sol > 0);
if isempty(R_sol)
      error('No valid footing radius found.');
end
R_final = max(R_guess, max(R_sol));           % m
D_final = 2 * R_final;                              % m

%% ---------------------------------------------------
% 4) ULTIMATE LOADS (ACI 318 FACTORED)
%% ---------------------------------------------------
Pu = 1.2*P_dead + 1.6*P_live;            % kN
Mux = 1.2*Mx_dead + 1.6*Mx_live;      % kN·m
```

```
Muy = 1.2*My_dead + 1.6*My_live;      % kN·m

%% ------------------------------------------------------
% 5) ITERATE FOR EFFECTIVE DEPTH (d)
%% ------------------------------------------------------
phi_f = 0.90;             % Flexure
phi_v = 0.85;              % Shear
d = d_init;               % Start with initial guess
d_step = 0.01;            % m, smaller step for precision
max_iter = 200;
iter = 0;
converged = false;

while iter <= max_iter
      iter = iter + 1;

      % Check validity of critical section
      if (c + 2*d) > 2*R_final
            error('c + 2d exceeds footing diameter at d=%.3f m.', d);
      end

      % 5A) CRITICAL MOMENTS (Your Original Equations)
      term = 4*R_final^2 - c^2;
      if term <= 0
            error('Invalid column size c=%.2f m for R=%.2f m.', c, R_final);
      end
      theta = asin(c/(2*R_final));

      % X-direction moment (Maa)
      F1 = (3*R_final^4*Pu*(0.5*(pi - sin(2*theta)) - theta) + Muy*(term)^1.5) / (3*pi*R_final^4);
      Xc_num = R_final^2*(Pu*(term)^1.5 + 3*Muy*R_final^2*(sin(4*theta) + 2*pi - 4*theta));
      Xc_den = 2*(3*R_final^4*Pu*(pi - 2*theta - sin(2*theta)) + 2*Muy*(term)^1.5);
      Xc = Xc_num / Xc_den;
      Maa = F1 * (Xc - c/2);    % kN·m

      % Y-direction moment (Mbb)
      F2 = (3*R_final^4*Pu*(0.5*(pi - sin(2*theta)) - theta) + Mux*(term)^1.5) / (3*pi*R_final^4);
      Yc_num = R_final^2*(Pu*(term)^1.5 + 3*Mux*R_final^2*(sin(4*theta) + 2*pi - 4*theta));
      Yc_den = 2*(3*R_final^4*Pu*(pi - 2*theta - sin(2*theta)) + 2*Mux*(term)^1.5);
      Yc = Yc_num / Yc_den;
      Mbb = F2 * (Yc - c/2);    % kN·m

      % 5B) FLEXURAL DEPTH CHECK
      M_control = max(Maa, Mbb);    % kN·m

      d_flex = (5*sqrt(M_control    / ( fc* R_final )))/1e3;      %m
      d = max(d, d_flex);

      % 5C) ONE-WAY SHEAR CHECK (Corrected Units)
      new_theta = asin((c + 2*d)/(2*R_final));
      V_term = 0.5*(pi - sin(2*new_theta)) - new_theta;
```

```
    % X-direction shear
    Vx_num = 3*R_final^4*Pu*V_term + Muy*(4*R_final^2 - (c+2*d)^2)^1.5;
    V_ee = Vx_num / (3*pi*R_final^4);    % kN

    % Y-direction shear
    Vy_num = 3*R_final^4*Pu*V_term + Mux*(4*R_final^2 - (c+2*d)^2)^1.5;
    V_ff = Vy_num / (3*pi*R_final^4);    % kN

    V_f = max(V_ee, V_ff);
    b_w_shear = sqrt(4*R_final^2 - (c + 2*d)^2);    % m
        v_oneway = phi_v * 0.17 *10^3* sqrt(fc) *b_w_shear*d;    %KN

    % 5D) PUNCHING SHEAR CHECK (Square Column)

    Qp = Pu - Pu * (c + d)^2 / (pi * R_final^2);    % kN
    v_punch_allow = phi_v * 0.33 * sqrt(fc)*10^3*(c+d)*4*d;

    % 5E) CONVERGENCE CHECK
    if V_f <= v_oneway && Qp <= v_punch_allow
        converged = true;
        break;
    else
        d = d + d_step;
    end
end

if ~converged
    error('Failed to converge in %d iterations.', max_iter);
end

%% ---------------------------------------------------
% 6) REINFORCEMENT DESIGN (ACI Minimum Enforced)
%% ---------------------------------------------------
final_thickness = d + cover;
concrete_volume = pi * R_final^2 * final_thickness;    % m³

% Minimum reinforcement (ACI 318 7.6.1.1)
  b_w = sqrt(4*R_final^2 - c^2);    % m
As_min = (1.4/fy)*b_w*d*1e6;    % mm²

% Required steel
z = 0.9 * d;
As_x = max((Maa * 1e6) / (phi_f * fy * z * 1e3), As_min);
As_y = max((Mbb * 1e6) / (phi_f * fy * z * 1e3), As_min);

%% ---------------------------------------------------
% 7) PRINT RESULTS
%% ---------------------------------------------------
fprintf('\n=== FINAL DESIGN ===\n');
fprintf('Footing Diameter:       %.2f m\n', D_final);
```

```
    fprintf('Effective Depth (d): %.3f m\n', d);
    fprintf('Total Thickness:          %.3f m\n', final_thickness);
    fprintf('Concrete Volume:          %.1f m³\n', concrete_volume);
    fprintf('X-Steel (As_x):           %.0f mm²\n', As_x);
    fprintf('Y-Steel (As_y):           %.0f mm²\n', As_y);
     fprintf('Shear V_ee:                  %.2f kN\n', V_ee);
    fprintf('Shear V_ff:                  %.2f kN\n', V_ff);
    fprintf('One-way shear allow: %.2f kN\n', v_oneway);
    fprintf('Punching shear Qp:      %.2f kN\n', Qp);
    fprintf('Punching shear allow:%.2f kN\n', v_punch_allow);
    fprintf('Moment Maa:                  %.2f kN·m\n', Maa);
    fprintf('Moment Mbb:                  %.2f kN·m\n', Mbb);
    fprintf('Iterations:                  %d\n', iter);

end


=== FINAL DESIGN ===
Footing Diameter:        3.89 m
Effective Depth (d): 0.420 m
Total Thickness:          0.495 m
Concrete Volume:          5.9 m³
X-Steel (As_x):           5856 mm²
Y-Steel (As_y):           6000 mm²
Shear V_ee:                 760.85 kN
Shear V_ff:                 778.91 kN
One-way shear allow: 1212.76 kN
Punching shear Qp:      2303.08 kN
Punching shear allow:2374.60 kN
Moment Maa:                796.83 kN·m
Moment Mbb:                816.42 kN·m
Iterations:                18
>>
```